# A combined SAXS/WAXS investigation of the phase behaviour of di-polyenoic membrane lipids

W. Patrick Williams [a,*], Beth A. Cunningham [b], D.H. Wolfe [c], Gareth E. Derbyshire [d], Geoff R. Mant [d], Wim Bras [d,e]

[a] Life Sciences Division, King's College London, Campden Hill, London W8 7AH, UK
[b] Department of Physics, Bucknell University, Lewisburg, PA 17837, USA
[c] Department of Astronomy and Physics, Lycoming College, Williamsport, PA 17701, USA.
[d] Daresbury Laboratory, Warrington, Cheshire WA4 4AD, UK
[e] Netherlands Organisation for Scientific Research (NWO), The Hague, The Netherlands

## Abstract

Real-time measurements of the SAXS/WAXS diffraction patterns of aqueous dispersions (1:1 wt/wt) of the di-polyenoic lipids di-18:2 PC, di-18:3 PC, di-18:2 PE and di-18:3 PE were made over the temperature range 10° to about −80°C. The results of these measurements were compared to similar measurements performed on the corresponding di-18:0 and di-18:1 derivatives. SAXS measurements of the temperature dependence of lamellar repeat distances show that the di-polyenoic lipids undergo broad second-order transitions between their gel and liquid-crystal lamellar phases spanning 30–40°C. The di-18:1 and di-18:0 derivatives, in contrast, undergo abrupt first-order transitions. The gel phases of the di-18:0 derivatives are characterised by two-component WAXS patterns with a sharp component close to 0.42 nm and a broader component at narrower spacings. On cooling, these lipids appear to undergo an initial transition to an $L_{\beta'}$ phase followed by a conversion to an $L_c$ phase. The gel phases of the di-18:1 derivatives also show two-component patterns but with the sharp component centred closer to 0.44 nm. The di-polyenoic lipids, in contrast, are characterised by a single broad peak centred at a spacing of about 0.42 nm, close to that of conventional $L_\beta$ phases. The changes in lamellar repeat distance accompanying the transitions in the di-monoenoic and di-polyenoic lipids, all of which occur in the frozen state, are very similar, indicating that the acyl chains of the polyenoic lipids are close to their maximum extension in the gel state. The WAXS patterns of the polyenoic lipids suggest that the saturated upper parts of the acyl chains are packed on a regular hexagonal lattice while their polyunsaturated termini remain relatively disordered.

Keywords: Phospholipid; Polyenoic lipid; X-ray diffraction; Lipid phase behaviour

## 1. Introduction

The response of cells and tissue to cryogenic temperatures is widely believed to be associated with the stability of biological membranes at low temperatures [1]. One of the common features of low-temperature adaptation in plants and micro-organisms exposed to low temperatures is to increase the degree of unsaturation of their membrane lipids [1–3]. This has led to an increasing interest in the low-temperature phase behaviour of membrane lipids.

Considerable information is available regarding the properties of mixed acid 1,2-diacyl-3-sn-phosphatidylcholines (PC), reflecting interest in the role of ω-3 polyunsaturated fatty acyl chains in the visual rod outer segment membranes and other neural membranes [4,5]. The phase properties of series of mixed-acid PC derivatives containing 16:0, 18:0 or 20:0 residues in the sn-1 position and polyenoic residues in the sn-2 position have been extensively studied using calorimetry [6–8], $^2$H NMR [9,10] and Raman spectroscopy [11].

The introduction of a single cis-double bond into the chain in the sn-2 position of di-18:0 PC lowers the temperature of the gel to liquid-crystal lamellar ($L_\beta$-$L_\alpha$) phase

---

Abbreviations: PC, phosphatidylcholine; PE, phosphatidylethanolamine; MGDG, monogalactosyldiacylglycerol; POPE 1-16:0, 2-18:1 phosphatidylethanolamine; $L_\alpha$, liquid-crystal lamellar phase; $L_\beta$, gel lamellar phase; $H_{II}$, inverted hexagonal phase; $L_c$, crystal (sub-gel) lamellar phase; $T_m$, gel to liquid-crystal phase transition temperature.
* Corresponding author. Fax: +44 171 333 4500.

transition, $T_m$, by about 50°C. A much smaller decrease is seen on introduction of a second cis-double bond. The introduction of further double bonds, in contrast, lead to small increases in $T_m$ [6,8]. A similar but more marked trend is seen in the molar enthalpies of the transitions. Related changes are seen in the values of $T_m$ of series containing C20 and C22 residues in the sn-2 position [8]. The transitions for most, but not all [8,10], of the lipids remain reasonably sharp, indicating a high degree of co-operativity.

Much less information is available regarding the properties of di-polyenoic lipids. The introduction of a second polyenoic chain has a very marked effect on the phase properties of membrane lipids. Keough and Kariel [12] showed that PC derivatives containing two identical poly-unsaturated chains are characterised by very broad, low enthalpy transitions starting at temperatures around −70°C and spanning ranges of approx. 40°C. We have confirmed and extended these observations using polyenoic phos-phatidylethanolamine (PE) [13] and monogalactosyldiacyl-glycerol (MGDG) [14] derivatives. These results suggest that membrane lipids containing two polyenoic chains form very disordered gel phases.

Preliminary X-ray diffraction studies tend to confirm this view [13,14]. Comparison of the low temperature wide-angle diffraction patterns of di-18:0, di-18:1 and di-18:2 PE indicated that the gel phase of the di-polyenoic lipid was much less ordered than that of the more saturated derivatives. The present investigation is aimed at providing a detailed high-resolution analysis of the low-temperature phase behaviour of di-polyenoic PC and PE derivatives. The work was carried out using the combined SAXS/WAXS facility recently installed at the Daresbury Laboratory Synchrotron, which offers a greatly improved accuracy in both the SAXS and WAXS regions as compared to earlier measurements.

## 2. Materials and methods

Di-18:0, di-18:1, di-18:2 and di-18:3 derivatives of PC and PE obtained from Avanti Lipids (Alabaster, Alabama) were used without further purification. Aqueous dispersions (1:1 wt/wt) were prepared by resuspending weighed amounts of lipid in distilled water. The lipid dispersions were prepared, as far as practical, in a $N_2$-filled glove box to minimise the chances of lipid oxidation. No significant differences were observed in the course of measurements using different batches of lipid measured on four separate occasions.

### 2.1. X-ray diffraction

Real-time X-ray diffraction measurements were conducted at station 8.2 of the Daresbury Synchrotron Radiation Source. A schematic diagram of the real-time SAXS/WAXS beamline is presented in Fig. 1. The optical system which forms the basis of the equipment, has been described in detail elsewhere [15,16].

The lipid samples were mounted in a 1-mm thickness cell fitted with mica windows attached to a modified THM 600 thermally-controlled microscope hot stage (Linkam, Tadworth (UK)) connected to a liquid-$N_2$ pump. Sample temperature was monitored using a thermocouple located in the sample cell. The SAXS pattern was measured above the direct beam using a standard Daresbury quadrant detector normally located at a distance of 3.2 meters. The WAXS pattern was measured below the direct beam using a commercially available curved INEL detector positioned so that the sample lies at the centre of its radius of curvature.

The data-acquisition system allowed 255 diffraction patterns to be collected consecutively with a 10 μs wait-time between patterns. The exposure time for each pattern,
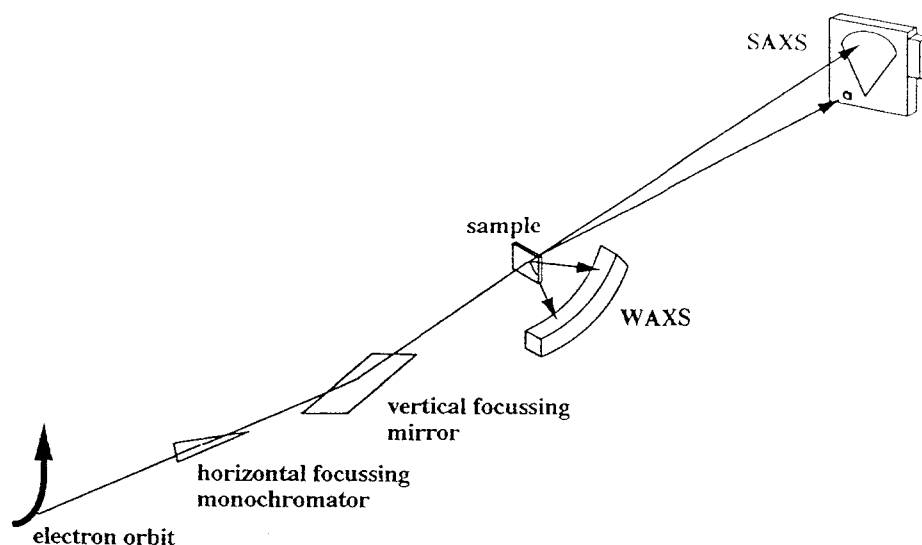


Fig. 1. Diagram showing the organisation of the SAXS/WAXS system.

unless otherwise noted, was 5 s. Samples were heated or cooled at a rate of $5°C \cdot min^{-1}$ giving a temperature resolution of better than 0.5°C. The quadrant detector was calibrated using the first nine orders of wet rat-tail collagen (repeat distance 67.0 nm). The INEL detector was calibrated using the peaks arising from hexagonal crystalline ice [17] present in the frozen samples as an internal standard.

## 3. Results

Real-time measurements were made of the SAXS/WAXS diffraction patterns of aqueous dispersions (1:1 wt/wt) of the polyenoic lipids di-18:2 PC, di-18:3 PC, di-18:2 PE and di-18:3 PE, the di-monoenoic lipids di-18:1 PC and di-18:1 PE and the fully saturated lipids di-18:0 PC and di-18:0 PE. The samples were cooled from 10° to $-80°C$ or lower at a rate of $5°C.min^{-1}$ and then reheated at the same rate.

### 3.1. SAXS measurements

The crucial difference between the behaviour of the more-saturated di-18:0 and di-18:1 and the more-unsaturated polyenoic di-18:2 and di-18:3 derivatives is highlighted in Fig. 2. The diagram contrasts the changes occurring in the position of the first-order lamellar repeat diffraction peaks of di-18:1 PE and di-18:3 PC in the course of the transition from the gel to the liquid-crystal state. The di-18:1 derivative is characterised by two distinct diffraction peaks centred at S = 0.173 and 0.192 $nm^{-1}$ (equivalent to lamellar repeat distances, d, of 5.78 and 5.21 nm) corresponding to the gel and liquid-crystal states, respectively. The transition, which is a classic first-order transition between two states, is largely completed in the course of ten 3-s frames. This correspond to a temperature range for co-existence of the two states of about 2.5°C, much of which can be accounted for in terms of temperature inhomogeneities in the sample.

The gel and liquid-crystal phases of the di-polyenoic lipids are also characterised by two diffraction maxima corresponding to the gel and liquid-crystal phase. In this case, the maxima are centred at $S = 0.18$ and 0.20 $nm^{-1}$ (equivalent to d-spacings of 5.6 and 5.0 nm). The transition is, however, clearly second order. It involves a continuous transition through a series of intermediate states reflected in the migration of the diffraction peak from its initial to its final position. This transition spans more than one hundred 5-s frames and corresponds to a temperature range of nearly 40°C.

In order to check that the presence of ice was not a major factor in determining transition width, the measurements on di-18:2 PC were repeated on a sample dispersed in aqueous ethylene glycol (66 wt%). Very similar results (not shown) to those observed in aqueous dispersions were obtained.

Plots of the temperature dependencies of the unit cell lengths calculated from the SAXS data obtained for the different PC and PE derivatives are shown in Fig. 3. Concentrated lipid dispersions of the type used in this study tend to exhibit extensive supercooling [18,19]. The data presented in Fig. 3 have, therefore, been calculated from heating runs to avoid complications associated with differences in the degree of supercooling occurring in different samples. The PC derivatives and di-18:0 PE are in lamellar phases over the whole temperature range. The unsaturated PE derivatives, however, form lamellar phases (indexing in the sequence 1:1/2:1/3:1/4....) in the frozen state and $H_{II}$ phases (indexing in the sequence $1:1/\sqrt{3}:1/\sqrt{4}:1/\sqrt{7}..$) in the unfrozen state. Only the first two maxima of the lamellar phases and the first three maxima of the $H_{II}$ phase were directly observable using the 3.2 m camera length. The phases were, therefore, independently indexed in control measurements using shorter camera lengths where more orders could be observed.

Collected values for the lamellar repeat distances for the gel and liquid-crystal phases of the different lipids are
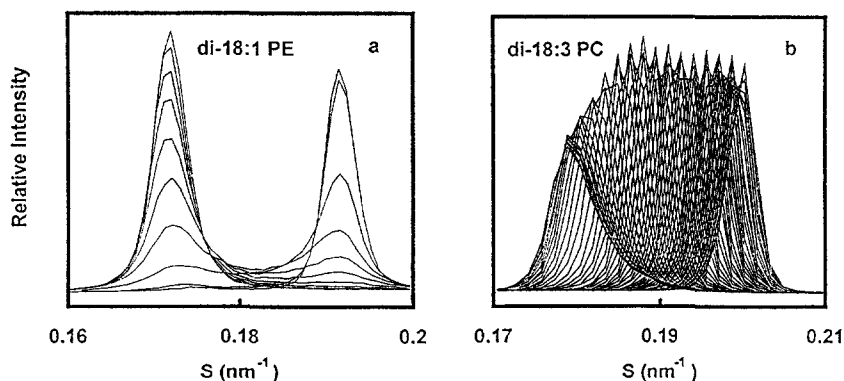


Fig. 2. Plots showing the change in position of the first order diffraction maxima on heating aqueous dispersions of (a) di-18:1 PE and (b) di-18:13 PC through their gel to liquid-crystal transition ranges at a rate of $5°C \cdot min^{-1}$. The individual patterns are alternate frames taken from a continuous series of 255 frames of 3 s duration in (a) and 5 s in (b). The frames span the temperature range $-7.4$ to $-2.4°C$ for di-18:0 PE and $-70$ to $-27°C$ for di-18:3 PC.
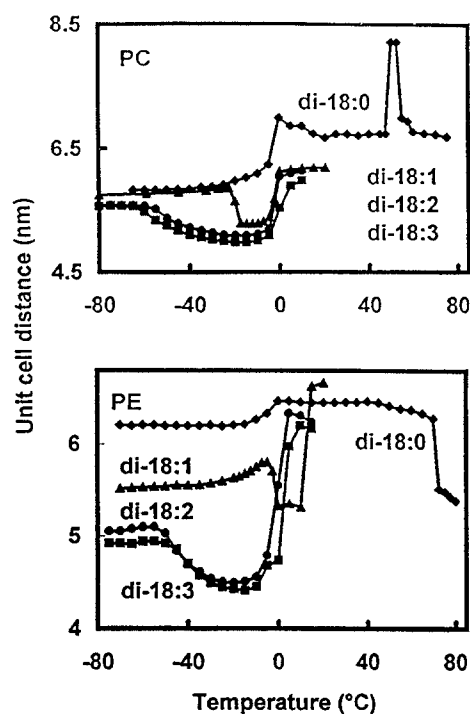
Fig. 3. Plots showing the temperature dependencies of the lamellar repeat spacings for aqueous dispersions (1:1 wt/wt) of (a) di-18:0 PC (♦), di-18:1 PC (▲), di-18:2 PC (●) and di-18:3 PC (■); and (b) di-18:0 PE (♦), di-18:1 PE (▲), di-18:2 PE (●) and di-18:3 PE (■), heated at a rate of 5°C·min⁻¹.

presented in Table 1. Homacyl-saturated derivatives of PC [20,21], and long-chain PE [29], tend to form gel phases in which the acyl chains are tilted with respect to the bilayer normal. For comparison purposes, therefore, measurements were also made for the mixed chain derivative 1-16:0, 2-18:1 PE (POPE) which forms a non-tilted gel phase. These results are also included in Table 1. Details of the temperatures at which the different transitions occur, and the ranges that they span, are provided in Table 2.

Table 1

Collected values of the lamellar repeat distance (d-spacing) values for the gel and lamellar liquid-crystal states of homoacyl di-18C derivatives of PC and PE

| Lipid | d-spacing (nm) | | |
|---|---|---|---|
| | Gel state | Liquid-crystal state | Δd |
| di-18:0 PC | 6.74 * | 6.69 | 0.05 |
| di-18:1 PC | 5.85 | 5.28 | 0.57 |
| di-18:2 PC | 5.57 | 5.09 | 0.48 |
| di-18:3 PC | 5.56 | 4.98 | 0.57 |
| di-18:0 PE | 6.28 | 5.50 | 0.78 |
| di-18:1 PE | 5.80 | 5.32 | 0.48 |
| di-18:2 PE | 5.09 | 4.50 | 0.59 |
| di-18:3 PE | 4.94 | 4.41 | 0.53 |
| 1-16:0,2-18:1 PE | 5.98 | 5.26 | 0.72 |

Spacings for the gel and liquid crystal phases were measured at temperatures just below and above the phase transition limits, respectively. Transitions, apart from those of di-18:0 derivatives, take place in ice.
* Gel spacing measured below pre-transition temperature.

Table 2

Collected values for the ranges and temperature spans of the gel to liquid crystal transitions of homoacyl di-18C derivatives of PC and PE

| Lipid | Transition Range (°C) | ΔT (°C) |
|---|---|---|
| di-18:0 PC | 54 to 55.5 | 1.5 |
| di-18:1 PC | − 18.4 to − 16.8 | 1.6 |
| di-18:2 PC | − 60 to − 28 | 32 |
| di-18:3 PC | − 64 to − 27 | 37 |
| di-18:0 PE | 71.2 to 74.7 | 3.5 |
| di-18:1 PE | − 6 to − 2.5 * | 3.5 |
| di-18:2 PE | − 53 to − 20 | 33 |
| di-18:3 PE | − 50 to − 22 | 32 |
| 1-16:0,2-18:1 PE | 23.8 to 25 | 1.2 |

* Transition in ice; corresponding values for transition in supercooled solutions were − 13.2° to − 11.8°C.

In the case of the unsaturated lipids, as illustrated in Fig. 3, all the lipids show large decreases in lamellar repeat distances on initial heating from low temperatures. The decreases seen in the monoenoic lipids are abrupt, occurring at about − 18°C for di-18:1 PC and about − 5°C for di-18:1 PE, and correspond to their well-documented gel to liquid-crystal lamellar transitions [13,19,22–24]. The decreases seen for the polyenoic lipids are of similar magnitude but span much larger temperature ranges. The onset values for the polyenoic PC derivatives obtained in this investigation are 5–10°C higher than those reported by Keough and Kariel [12] on the basis of DSC measurements, but the overall span of the transitions are broadly similar.

These initial decreases are followed by large increases in repeat distance starting slowly at about − 15°C and rapidly increasing as the temperature of the samples approaches 0°C. These reflect the rehydration of the lipid samples as the ice within the frozen samples remelts [18,19]. In the case of the unsaturated PE derivatives, as we have discussed elsewhere [18], this melting process is accompanied by a simultaneous transition from the $L_\alpha$ phase to the $H_{II}$ phase.

The pattern of changes occurring in the saturated lipids is quite different. The lipids are still in the gel phase at 0°C and the increases in lamellar repeat distance associated with the melting of ice, particularly for di-18:0 PE, tend to be smaller than those seen for the unsaturated lipids. The decrease in lamellar repeat distance accompanying their gel to liquid-crystal transitions occurs at much higher temperatures. In the case of di-18:0 PC, it is preceded by a large increase in spacing, occurring between 50° and 54°C, reflecting the formation of the ripple ($P_{\beta'}$) phase [25,26].

The low-temperature changes shown in Fig. 3 are fully reversible. This is illustrated by the direct comparison of the temperature dependencies of lamellar repeat spacing calculated from cooling and heating runs for di-18:3 PE presented in Fig. 4. Little hysteresis is observed, indicating that the measurements were made under near-equilibrium conditions.

## 3.2. WAXS measurements

Gel states are normally characterised by a high degree of organisation of their acyl chains. One of the difficulties associated with the characterisation of the low-temperature state of the di-polyenoic lipids has been the comparative lack of order revealed in existing wide-angle diffraction measurements of such lipids [13,14].

Representative examples of the WAXS diffraction patterns of the di-18:0, di-18:1 and di-18:2/di-18:3 derivatives of PC and PE obtained in this study are shown in Figs. 5–8.

In the case of the saturated lipids, as the samples are cooled, the sharp diffraction maximum centred at a spacing of about 0.42 nm ($2\Theta = 21.18°$), typical of the hexagonal lattice of the $L_\beta$ state, splits into a sharp component which remains close to 0.42 nm and a broad component centred at a narrower spacing. Comparison of the WAXS patterns of di-18:0 PC in the cooling sequence shown in Fig. 5a with the WAXS patterns of low-temperature stored di-16:0 PC reported by Ruocco and Shipley [27] suggests that the lipid first passes through a quasi-hexagonal $L_{\beta'}$ phase in which the acyl chains are tilted at an angle to the bilayer normal and then, at lower temperatures, enters a $L_c$ phase. The WAXS pattern collected at $-8°C$, for the supercooled dispersion just prior to ice formation, is shown in more detail in Fig. 6a. It consists of a sharp reflection at 0.428 nm ($2\Theta = 20.78°$) and a broader maximum centred at about 0.393 nm ($2\Theta = 22.67°$). This compares to spacings of 0.44 and 0.39 nm reported for the $L_c$ phase of di-16:0 PC [27].

Similar changes in the WAXS diffraction patterns of di-18:0 PE are shown in Fig. 5b,c. In this case, the diffraction peak is very sharp at temperatures just below the gel to liquid-crystal transition suggesting that the lipid forms a classic $L_\beta$ phase under these conditions. It is much broader at temperatures below about 30°C and again splits into two components when cooled to lower temperatures. Just prior to ice formation, the main diffraction peak and the broad maximum, as illustrated in Fig. 6b, are located at



Fig. 5. Typical WAXS diffraction patterns of aqueous dispersions of (a) di-18:0 PC cooled from 63° to $-17°C$, (b) di-18:0 PE cooled from 10° to $-10°C$ and (c) di-18:0 PE and heated from 10° to 76°C. Heating/cooling rates were $5°C \cdot min^{-1}$. Sharp peaks appearing in (a) on cooling to $-17°C$ arise from hexagonal ice.
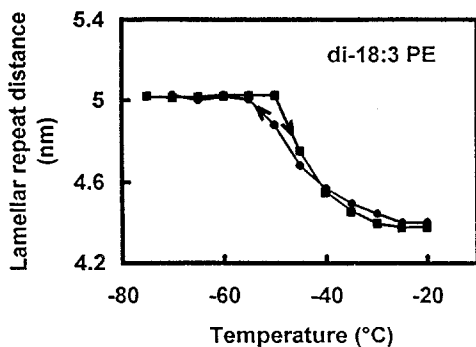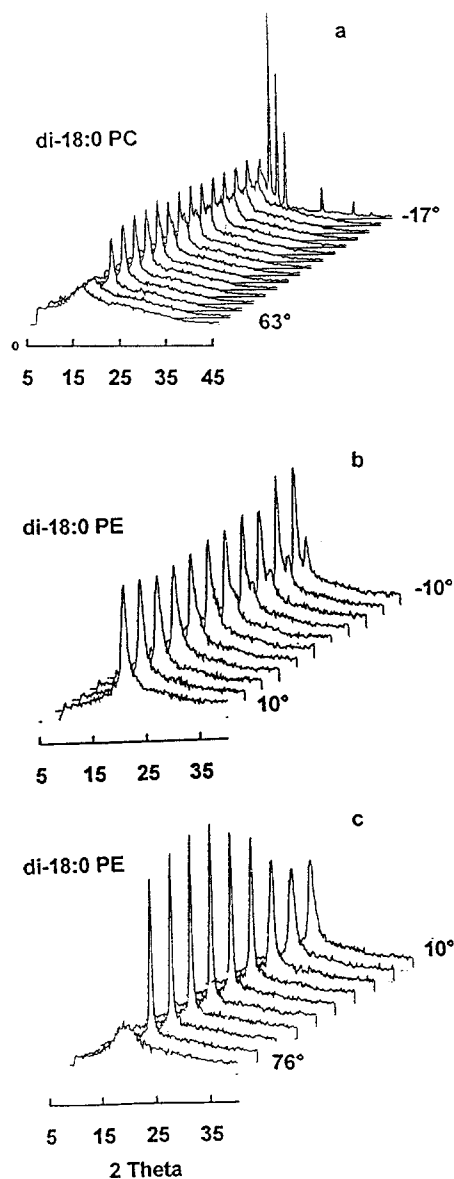


Fig. 4. Plots showing the temperature dependencies of the lamellar repeat spacings for an aqueous dispersions (1:1 wt/wt) of di-18:3 PE cooled (●) and then reheated (■) at a rate of $5°C \cdot min^{-1}$.

0.415 nm ($2\Theta = 21.45°$) and 0.381 nm ($2\Theta = 23.35°$). These values are in good agreement with the values of 0.418 and 0.388 nm for a crystal form of this lipid reported by Harlos [28].

The similarity of the pattern of changes for di-18:0 PE and di-18:0 PC shown in Fig. 5 suggests that di-18:0 PE also forms an $L_{\beta'}$ phase prior to entering the $L_c$ phase. This is in agreement with work of Seddon et al. [29] suggesting that saturated homoacyl derivatives of PE with chain lengths of $C_{18}$ or greater are capable of forming $L_{\beta'}$ phases.
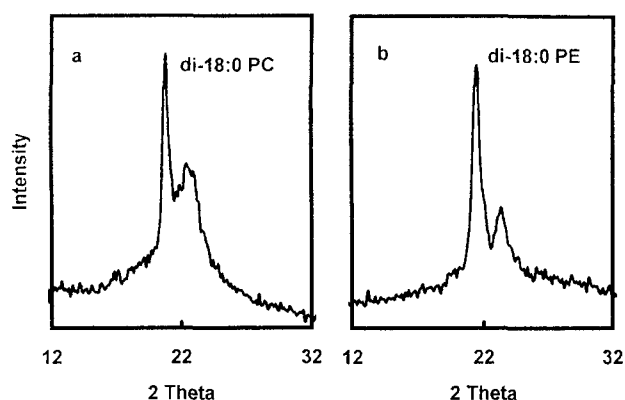
Fig. 6. WAXS diffraction patterns of (a) di-18:0 PC and (b) di-18:0 PE measured at $-8°$ and $-9°C$ in supercooled dispersions just prior to sample freezing.

A similar splitting of WAXS maxima is observed for the di-monoenoic lipids (Fig. 7a,b). In these lipids, the main component is shifted to a wider spacing, 0.438 and 0.445 nm ($2\Theta = 20.3°$ and $20.0°$) for di-18:1 PC and di-18:1 PE, respectively. The low transition temperatures of these lipids means that they commonly freeze prior to the gel to liquid-crystal transition and many of the features of their WAXS patterns tend to be obscured by the presence of the three sharp diffraction peaks centred at $2\Theta = 22.8°$, $24.2°$ and $26.0°$ arising from the (100), (002) and (101) reflections of hexagonal crystalline ice [17].

This problem can be avoided by the use of samples containing reduced water contents. A typical low temperature WAXS pattern for di-18:1 PC is presented in Fig. 8a. However, despite the fact that the ice peaks are largely suppressed, the precise position of the broader diffraction

maximum at narrower spacings is still difficult to determine. WAXS patterns for a comparable sample of di-18:0 PC are shown in Fig. 8b. In this case, the pattern collected at $-8°C$ is similar to that obtained for the fully-hydrated supercooled sample shown in Fig. 6a. The pattern collected at $-40°C$, however, is much closer to that expected for an $L_{\beta'}$ phase [27], suggesting that freeze-dehydration might have some effect on the ability of the lipid to enter an $L_c$ phase.

In contrast to the di-18:0 and di-18:1 derivatives, the di-polyenoics show no indication of any splitting in their WAXS patterns (Fig. 7c). The broad diffraction maximum centred at about $2\Theta = 19.8°$ (d = 0.45 nm), typical of the liquid-crystal state, simply migrates to shorter spacings and sharpens as the temperature is lowered and the sample enters the gel phase. A typical low-temperature WAXS diffraction pattern for a polyenoic lipid (di-18:2 PC) dispersed in reduced amounts of water is compared to that of a similar sample of the mixed chain lipid 1-16:0,2-18:1 PE, which forms a conventional $L_\beta$ phase, in Fig. 8c. In both cases the diffraction peak associated with the packing of the acyl chains is symmetric. The positions of the two diffraction maxima are very similar but the peak for the polyenoic lipid is much broader showing that the chains are much less well-organised.

In order to check whether this broadening is simply a reflection of freeze-dehydration, the effects of cooling on the WAXS diffraction pattern of 1-16:0,2-18:1 PE were examined. As illustrated in Fig. 9, very low temperatures do lead to some broadening of the diffraction maximum. The degree of broadening from this source is, however, relatively modest.
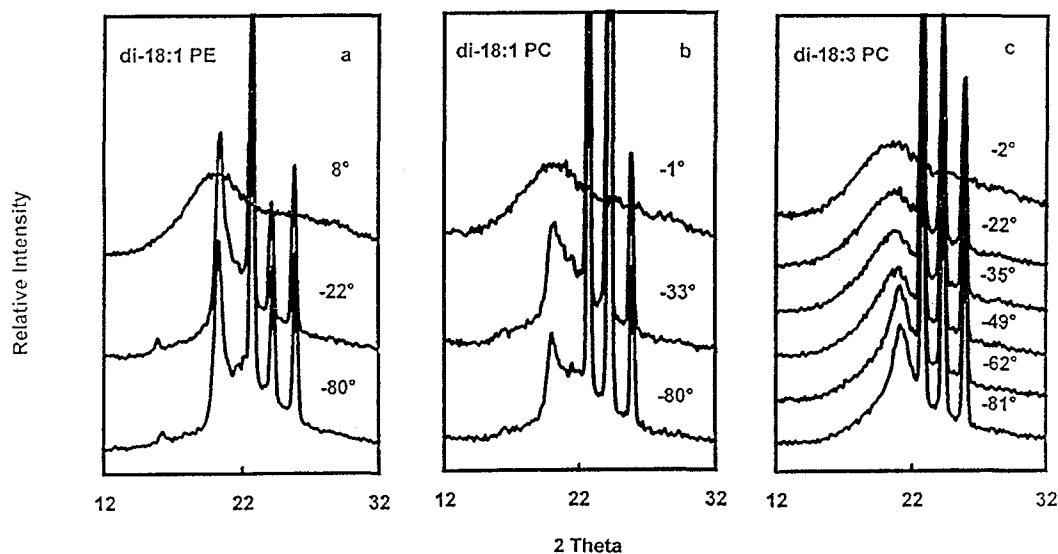


Fig. 7. Typical low temperature WAXS diffraction patterns of aqueous dispersions of (a) di-18:1 PE, (b) di-18:1 PC and (c) di-18:3 PC at indicated temperatures. The three sharp peaks correspond to diffraction maxima of hexagonal ice.

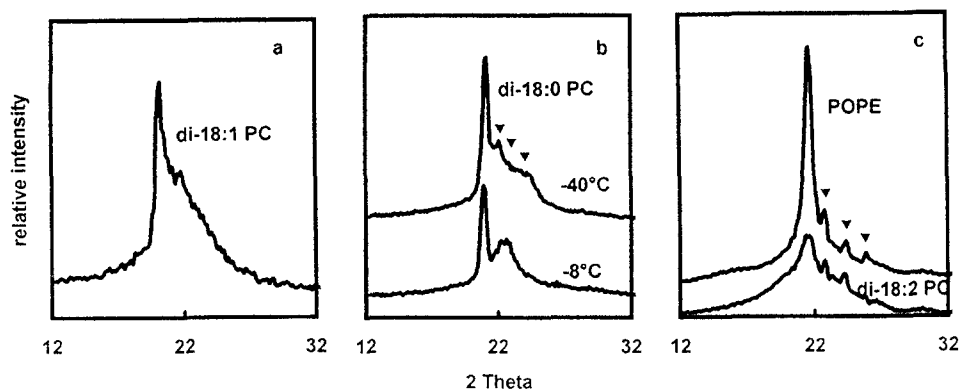W.P. Williams et al. / Biochimica et Biophysica Acta 1284 (1996) 86–96



Fig. 8. Low temperature WAXS diffraction patterns of aqueous dispersions containing reduced amounts of water (lipid:water, 1:0.25 wt./wt.,) of (a) di-18:1 PC measured at −40°C, (b) di-18:0 PC measured at −8° and −40°C, (c) di-18:2 PC and 1-16:0,2-18:1 PE (POPE) measured at −90°C. Arrows indicate position of residual ice maxima.

Plots of the temperature dependencies of the main WAXS diffraction spacing of the different PC and PE derivatives are presented in Figs. 10 and 11. In the case of the saturated lipids, the main changes, occurring at about 54° and 75°C, are clearly associated with the gel to liquid-crystal transitions of the two lipids. The slightly wider spacing of the main component of the WAXS pattern of di-18:0 PC at low temperatures, 0.424 nm as opposed to 0.415 nm for di-18:0 PE, reflects differences in the organisation of their low temperature phases. The changes in spacing occurring between about −30°C and 20°C reflect the changes in the WAXS patterns of the two lipids illustrated in Figs. 5 and 8b.

In the case of the unsaturated lipids, the changes in the WAXS region closely mirror those illustrated for the SAXS region in Fig. 2. The transition between the gel and liquid-crystal state in the polyenoic lipids again consists of a continuous process in which the position of the diffrac-

tion maximum gradually shifts from a spacing typical of the fully-formed gel state at temperatures below −70°C to that typical of the liquid-crystal state at temperatures above about −20°C. The plots are clearly sigmoidal, indicating that the transitions are not simple reflections of thermal expansion. The temperature coefficient increases from a value of about $5.0 \times 10^{-5}$ nm.°C$^{-1}$ in the gel state to a maximal value of about $1.1 \times 10^{-3}$ nm.°C$^{-1}$ in the transition region before falling back to about $1.6 \times 10^{-4}$ nm.°C$^{-1}$ in the $L_\alpha$ phase.

It is noteworthy that the onset temperatures for the transitions occurring in the polyenoic lipids as reflected in the WAXS spacings are a little lower than those reflected in the d-spacing data shown in Fig. 3 and listed in Table 2. This indicates that the organisation of the acyl chains is still changing even after the chains have reached their greatest extension. It is possibly these minor changes that account for the rather lower onset temperatures reported in the DSC measurements of Keough and Kariel [12] as compared to the d-spacing measurements.
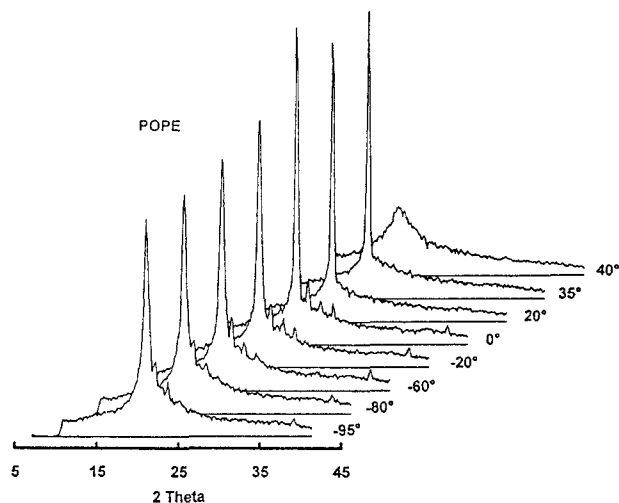


Fig. 9. WAXS diffraction patterns of aqueous dispersions of 1-16:0,2-18:1 PE (POPE) (lipid:water, 1:0.25 wt/wt) showing the broadening of the diffraction maximum associated with acyl chain packing at low temperatures.
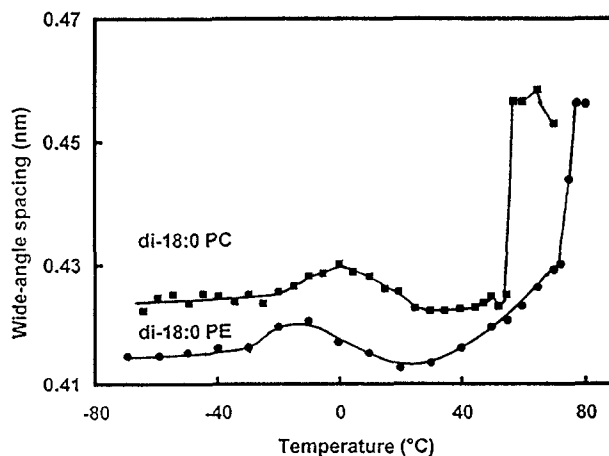


Fig. 10. Plot showing the temperature dependencies of the WAXS spacings associated with the packing of the acyl lipid chains of aqueous dispersions (1:1 wt/wt) of di-18:0 PC () and di-18:0 PE () and (b) heated at a rate of 5°C·min$^{-1}$.

The behaviour of the di-monoenoic lipids is rather more complex. Only the position of the main component of the WAXS diffraction pattern is plotted in Fig. 11 as the exact position of the smaller component (shoulder) is difficult to resolve in the presence of ice. In both cases, the spacing of the main component shows a gradual reduction as the gel-phase lipids approach their phase transition temperatures. As illustrated in Fig. 3, this reduction is accompanied by an increase in lamellar repeat distance. These changes, which are particularly marked for di-18:1 PE, may reflect decreases in the angle of tilt of the lipid chains. This view is supported by the WAXS diffraction patterns for samples of di-18:1 PE and PC with reduced water content presented in Fig. 12. These patterns show clear indications of the existence of intermediates characterised by a single broad diffraction maximum at temperatures just below that of their gel to liquid-crystal phase transition (cf. Fig. 7c and 8b). The acyl chains of the di-18:1 derivatives, like those of di-18:0 PE, appear to straighten just prior to entering the liquid-crystal phase. Unlike di-18:0 PE, however, the chains of the di-monoenoic lipids are unable to
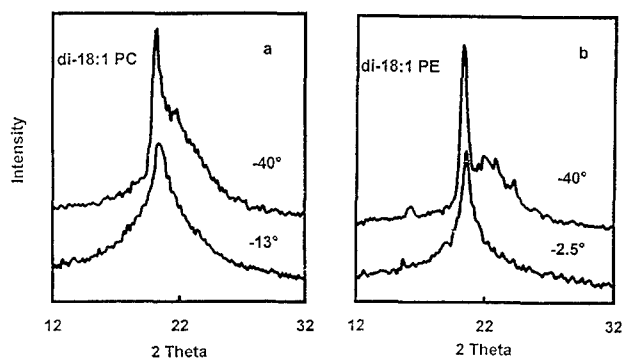


Fig. 12. WAXS diffraction patterns of aqueous dispersions of (a) di-18:1 PE and (b) di-18:1 PC in low amounts of water (lipid:water 1:0.1 wt/wt) measured at indicated temperatures.

form a well-ordered hexagonal lattice under these conditions and give rise to broad maxima, resembling those of the di-polyenoic lipids, rather than the sharp maximum seen for the fully-saturated lipid.

## 4. Discussion

This study deals with the low temperature phase behaviour of homoacyl lipids of different degrees of saturation. The effects of the formation and melting of ice on the repeat distance of lamellar phases and the stability of $H_{II}$ phases have been dealt with in some detail elsewhere [13,17,18] and will not be further considered here. Attention will be confined to changes associated with the gel to liquid-crystal lamellar phase transitions occurring in the different lipids and the packing of the acyl chains in the gel phases of such lipids.

X-ray diffraction measurements provide valuable information about three aspects of these problems. Firstly, measurements in the SAXS region provide data on the lamellar repeat distance and hence on the degree of extension of the lipid chains in the different phases. Secondly, measurements in the WAXS region provide information about the packing and possible angle of tilt of the acyl chains in such phases. Finally, the fact that the measurements are carried out in real time provides information both about the reversibility and co-operativity of the phase transitions. Each of these aspects will be discussed in turn.

### 4.1. Lamellar repeat distances

The temperature dependencies of the d-spacing of the different lipids are shown in Fig. 3. The changes in repeat distance, $\Delta d$, associated with their gel to liquid-crystal phase transitions, and the temperature ranges over which these changes occur, are summarised in Tables 1 and 2.

In general, changes in d-spacing reflect changes in lipid bilayer thickness and/or the thickness of the water layer
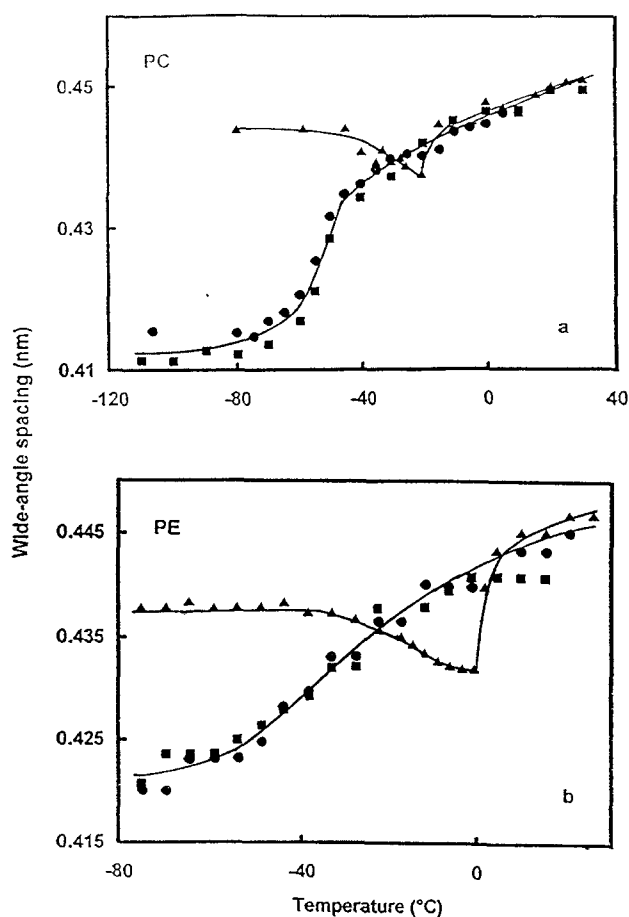


Fig. 11. Plots showing the temperature dependencies of the WAXS spacings associated with the packing of the acyl lipid chains of aqueous dispersions (1:1 wt/wt) of (a) di-18:1 PC (▲), di-18:2 PC (●) and di-18:3 PC (■), (b) di-18:1 PE (▲), di-18:2 PE (●) and di-18:3 PE (■). All samples were heated at a rate of 5°C·min⁻¹.

between the bilayers. The thickness, and the rate of change in the thickness with temperature, of the unfrozen water layer between adjacent bilayers in frozen samples of hydrated di-18:1 PC have been investigated by Gleeson et al. [19]. They estimated the thickness of this layer to be about 0.4 nm at $-15°C$. Its rate of change with temperature was found to be very low, below about $-10°C$. This suggests that the $\Delta d$ values seen in our frozen samples, in the first approximation at least, can be taken as direct reflections of changes in bilayer thickness.

The measured difference in d-spacing on going from the gel state to the liquid-crystal state in the different polyenoic samples varies between 0.48 and 0.59 nm. The corresponding values for di-18:1 PC and di-18:1 PE were 0.57 and 0.48 nm, respectively. It is clear, therefore, that the polyenoic chains must be close to their maximal extension at temperatures below about $-60°C$ in our experiments.

## 4.2. Acyl chain packing

Our WAXS diffraction measurements indicate major differences in the acyl chain packing of di-saturated, di-monoenoic and di-polyenoic derivatives of PC and PE. Apart from di-18:0 PE at temperatures close to its gel to liquid-crystal phase transition, none of these lipids show the single sharp diffraction peak located at a spacing of about 0.42 nm associated with a conventional $L_\beta$ phase in which the acyl chains are packed parallel to the bilayer normal on a regular hexagonal lattice.

Saturated homoacyl PC derivatives like di-18:0 PC, are well known to form quasi-hexagonal $L_{\beta'}$ phases on cooling below their pre-transition range [20,21]. Seddon et al. [29] have reported a similar tilted $L_{\beta'}$ phase for di-20:0 PE and suggest that such phases are a common feature of homoacyl di-saturated PE derivatives with chain lengths of $C_{18}$ or more. This behaviour contrasts with shorter chain homologues such as di-16:0 PE where the chains pack parallel to the bilayer normal in the gel phase [30].

The homoacyl derivatives of PC and PE are known to form well-defined $L_c$ phases characterised by two, or more, reflections in the WAXS region. Ruocco and Shipley [27] report spacings of 0.44 and 0.39 nm for the main component and the less intense broader diffraction maximum of an $L_c$ phase of hydrated di-16:0 PC. The corresponding values for the $L_{\beta'}$ phase, the stable gel form at higher temperatures, are a main reflection at 0.42 nm with a shoulder at about 0.41 nm. Our di-18:0 PC samples show a progressive splitting of their main WAXS diffraction peak (Fig. 5a). Just prior to ice formation, the main component is centred at 0.428 nm and the broader subsidiary maximum at 0.393 nm. This is consistent with an initial conversion to an $L_{\beta'}$ phase followed by conversion, or partial conversion, to the $L_c$ phase. $L_c$ phase formation occurs much more readily in di-18:0 PC than in di-16:0 PC, which requires a period of low temperature storage [31].

This probably reflects the greater capacity for inter-chain Van der Waals interactions in the longer chain lipid.

Similar changes are seen in the WAXS pattern of our di-18:0 PE samples (Fig. 5b). In this case, the spacings of the two components of the WAXS pattern just prior to freezing are 0.415 nm and 0.381 nm; in good agreement with the values of 0.418 and 0.388 nm reported by Harlos [28]. Harlos attributed this splitting of the WAXS pattern to an anisotropic expansion of an originally hexagonal acyl chain lattice resulting in its conversion to a rectangular I symmetry. Other measurements, however, suggest that the acyl chain packing of di-18:0 PE and its analogues is more complex [32–34] and that their chains are packed on some form of hybrid orthorhombic sub-cell similar to that proposed by Ruocco and Shipley [27] for di-16:0 PC.

The WAXS diffraction patterns of the di-monoenoic lipids show a similar splitting to that seen in the fully saturated lipids but in their case the sharp component is displaced to a wider spacing (Figs. 8 and 11). Lewis et al. [35] have presented detailed calorimetric and $^{31}P$ NMR data, suggesting that di-18:1 PC first forms an $L_{\beta'}$ phase on entering the gel phase which then converts to a disordered $L_c$ phase. They point out that the presence of substituents near the methyl terminus of the acyl chain appears to promote the formation of condensed $L_c$-like phases in PC bilayers and suggest that di-monoenoic lipids might be thought of in this context as short-chain alkanoics with bulky 1,2-cis-decenyl groups attached to their ω-carbon atoms.

A minor component at a spacing close to 0.56 nm $(2\Theta = 15.8°)$ is clearly visible in the WAXS diffraction patterns of di-18:1 PE shown in Figs. 7 and 12. Similar, more prominent, peaks are seen in the $L_c$ phase of di-18:1 PE formed in DMSO dispersions [36]. The homoacyl di-monoenoic lipids, like the di-saturated lipids thus appear to be entering, or attempting to enter an $L_c$, phase in the gel state. The requirement to accommodate their 1,2-cis-decenyl groups appears to be a greater driving force than that experienced by the di-saturated lipids leading to a more rapid, and possibly more complete, transfer to this state within the timescale of our measurements.

The di-18:2 and di-18:3 derivatives of PC and PE, in contrast, show no indication of $L_c$ phase formation. The 1,4-pentadiene and/or 1,4,7-octatriene groups present in their acyl chains greatly increases the number of gauche transitions. This presumably reduces the number of methylene group hydrogens available to participate in Van der Waals interactions between neighbouring chains to such an extent that there is insufficient driving force to form such phases. It should be emphasised that the presence of polyenoic chains in both the sn-1 and sn-2 positions does not of itself preclude the formation of highly-ordered lattices. As we have shown elsewhere [14], di-18:3 MGDG is capable of forming a well-ordered $L_c$ phase. In this case, however, it is the formation of an extensive hydrogen bonding network between the sugar headgroups of the

lipid rather than Van der Waals interactions between the acyl chains that is the driving force for acyl chain alignment.

The WAXS diffraction maxima for the gel phases of the di-polyenoic lipids are much more symmetrical than those for the di-saturated and di-monoenoic lipids (Figs. 7 and 8). Their central position is also very close to that of a conventional $L_\beta$ phase. The breadth of the peaks, however, clearly indicates the lack of uniformity in the packing of the acyl chains in such phases. This can most easily be accounted for on the basis of an ordering of the short saturated sections of the acyl chains into a regular hexagonal lattice with the polyenoic tails, which are characterised by the presence of multiple *gauche* conformers, still in a relatively disorganised state.

This type of organisation is similar to that suggested by the model used by Cevc [37] for the prediction of the $T_m$ values of membrane lipids. This model is based on the idea that $T_m$ is largely determined by the longest length of continuous adjacent saturated acyl chain capable of forming all-*trans* conformers and hence available to form effective inter-chain Van der Waals interactions. The unsaturated regions, it is assumed, are relatively disorganised and contribute little to gel phase stability. Cevc has developed equations for calculating the effective chain length ($n_{ef}$) of different unsaturated chains and has shown that the $T_m$ value of any unsaturated lipid approximates closely to that of the corresponding di-saturated derivative with chains of that length.

In the case of the polyenoic PC derivatives, the model predicts $T_m$ values of $-58°$ and $-67°C$ for di-18:2 and di-18:3 PC, respectively. These values are very similar to our values of $-60°$ and $-64°C$ for the onset of the gel to liquid-crystal phase transition of these two lipids. The $T_m$ values predicted by Cevc correspond to $n_{ef}$ values of 8.78 and 9.09, close to the number of carbon atoms per chain in the main saturated sections of these lipids, emphasizing the minimal contribution of the polyunsaturated chain termini.

## 4.3. Co-operativity

The high degree of co-operativity characteristic of most gel to liquid-crystal transitions in lipids reflects the fact that free rotation around the single C-C bonds of such chains involves the simultaneous disruption of the many Van der Waals interactions stabilising the regular hexagonal lattice (or in the case of $L_{\beta'}$ phases, the quasi-hexagonal lattice) formed by the acyl chains in the gel state. Transitions of this type are characterised by two distinct states which have equal stability at the transition temperature resulting in a two-state transition of the type illustrated in Fig. 2a.

The presence of polyenoic acyl chains has a destabilising effect both on the gel and liquid-crystal phases of membrane lipids [6]. The stability of the gel state is lowered by the reduction in strength of the Van der Waals

interactions between neighbouring chains due to the large number of *gauche* conformers associated with their multiple *cis*-double bonds. At the same time the presence of these bonds reduces the number of attainable *gauche-trans* isomerisations in the fluid state. The net result of these two effects, as detailed by Coolbear et al. [6], is a tendency to reduce the disparity between these two states and hence reduce the degree of co-operativity of the transition between them. In the case of di-polyenoic lipids, as illustrated in Fig. 2b, there is an almost total loss of co-operativity and the normal first order transition is replaced by a second order transition involving a continuum of stable intermediate states.

## References

[1] Morris, G.J. (1987) in The Effects of Low Temperatures on Biological Systems (Grout, B.W.W. and Morris, G.J., eds.), pp. 120–146, Edward Arnold, London.

[2] Oquist, G. (1983) Plant Cell Environ. 6, 281–300.

[3] Russell, N.J. (1990) Phil. Trans. R. Soc. Lond. B326, 595–611.

[4] Milijanich, G.P., Sklar, L.A., White, D.L. and Dratz, E.A. (1979) Biochim. Biophys. Acta 552, 294–306.

[5] Salem, N.J. (1989) In Current Topics in Nutrition and Disease (Spiller, G.A. and Scala, J., eds.), pp. 109–228, Alan R. Liss, New York.

[6] Coolbear, K.P., Berde, C.B. and Keough, K.M.W. (1983) Biochemistry, 22, 1466–1473.

[7] Keough, K.M.W., Giffin, B. and Kariel, N. (1987) Biochim. Biophys. Acta 902, 1–10.

[8] Niebylski, C.D. and Salem, N. (1994) Biophys J. 67, 2387–2393.

[9] Barry, J.A., Trouard, T.P., Salmon, A. and Brown, M.F. (1991) Biochemistry 30, 8386–8394.

[10] Holte, L.L., Peter, S.A., Sinnwell, T.M. and Gawrisch, K. (1995) Biophys. J. 68, 2396–2403.

[11] Litman, B.J., Lewis, E.N. and Levin, I.W. (1991) Biochemistry 30, 313–319.

[12] Keough, K.M.W. and Kariel, N. (1987) Biochim. Biophys. Acta 902, 11–18.

[13] Williams, W.P., Sanderson P.W, Cunningham, B.A., Wolfe D.H. and Lis, L.J. (1993) Biochim. Biophys. Acta 1148, 285–290.

[14] Sanderson, P.W. and Williams, W.P. (1992) Biochim. Biophys. Acta 1107, 77–85.

[15] Bras, W., Derbyshire, G.E., Ryan, A.J., Mant, G.R., Manning, P., Cameron, R.E. and Mormann, W. (1993) J. Physique IV 3, 447–450.

[16] Cunningham, B., Quinn, P.J. and Bras, W. (1994) J. Biochem. Biophys. Methods 29, 87–111.

[17] Dowell, L.G., Moline, S.W. and Rinfret, A.P. (1962) Biochim. Biophys. Acta 59, 229–242.

[18] Sanderson, P.W, Williams, W.P., Cunningham, B.A., Wolfe, D.H. and Lis, L.J. (1993) Biochim. Biophys. Acta 1148, 278–284.

[19] Gleeson, J.T., Erramilli, S. and Gruner, S.M. (1994) Biophys. J. 67, 708–712.

[20] Tardieu, A., Luzzati, V. and Reman, F.C. (1973) J. Mol. Biol. 75, 711–733.

[21] Ranck, J.L. (1983) Chem. Phys. Lipids, 32, 251–270.

[22] Phillips, M.C., Williams, R.M. and Chapman, D. (1969) Chem. Phys. Lipids 3, 234–244.

[23] Barton, P.G. and Gunstone, F.D. (1975) J. Biol. Chem. 250, 4470–4476.

[24] Silvius, J.R. and McElhaney, R.N. (1979) Chem. Phys. Lipids, 25, 125–134.

[25] Janiak, M.J., Small, D.M. and Shipley, G.G. (1976) Biochemistry 15, 4575–4580.

[26] Yu, Z-W. and Quinn, P.J. (1996) Biophys. J. 69, 1456–1463.

[27] Ruocco, M.J. and Shipley, G.G. (1982) Biochim. Biophys. Acta 684, 123–132.

[28] Harlos, K. (1978) Biochim. Biophys. Acta 511, 348–355.

[29] Seddon, J.M., Cevc, G., Kaye, R.D. and Marsh, D. (1984) Biochemistry 23, 2634–2644.

[30] McIntosh, T.J. (1980) Biophys. J. 29, 237–246.

[31] Chen, S.C., Sturtevant, J.M. and Gaffney, B.J. (1980) Proc. Natl. Acad. Sci. USA 77, 5060–5063.

[32] Seddon, J.M., Harlos, K. and Marsh, D. (1983) J. Biol. Chem. 258, 3850–3854.

[33] Tenchov, B.G., Lis, L. and Quinn, P.J. (1988) Biochim. Biophys. Acta 942, 305–314.

[34] Williams, W.P., Quinn, P.J., Tsonev, L.I and Koyonova, R.D. (1991) Biochim. Biophys. Acta 1062, 123–132.

[35] Lewis, R.N.A.H., Sykes, B.D. and McElhaney, R.N. (1988) Biochemistry 27, 880–887.

[36] Yu, W-Z., Williams, W.P. and Quinn, P.J. (1996) Arch. Biochem. Biophys., in press.

[37] Cevc, G. (1991) Biochemistry 30, 7186–7193.